

CFD Simulation of Solar Air Heater having Inclined Discrete Rib Roughness with Staggered Element

Mahendra Kumar Ahirwar¹, K R Aharwal²

¹MTech student, Thermal Engineering, Maulana Azad National Institute of Technology, Bhopal, India

²Professor, Dept. of Mechanical Engineering, Maulana Azad National Institute of Technology, Bhopal, India

Abstract - In this study 3-D CFD simulations are done to investigate heat transfer and fluid flow characteristics of artificially roughened duct using Ansys-Fluent. We saw how Reynolds number affects the Nusselt number. The air flow has been computed in terms of Reynolds numbers ranging from 6000 to 12000 using the finite volume approach and the SIMPLE algorithm. The roughness pitch to rib height ratio ranged from 6 to 12, the length of staggered element to gap width ratio was 2, the relative staggered position was 0.6, and the width of the gap to roughness height ratio was 1. The Nusselt number, flow friction, and thermal performance of the rectangular channel with inclined rib staggered arrangement were compared to inclined rib with a staggered element. The staggered element increases the turbulence intensity in its vicinity, resulting in increased heat transfer and so strengthening the flow. A commercial bundle with a limited volume software ANSYS FLUENT R1 2021 is used to analyse and visualise the flow over the duct of a solar air heater. The geometry of the model is created in design modeller, then meshed, analysed, and post-processed with Ansys-fluent R1 software. Heat transfer and fluid flow are simulated and compared using a turbulent flow model (RNG k -), using steady-state solvers to determine pressure drop, flow, and temperature fields. The duct's bottom wall is roughened by various geometries of discrete ribs. The heat transfer simulation results for different roughness configurations varies slightly, and the Ansys-Fluent programme was used to simulate the flow fields in a rectangular duct. CFD simulation results were found almost close to the experimental results and with the standard theoretical approaches. We found that the Nusselt number increases with increase in Reynolds number. The maximum increment in Nusselt number and friction factor is 3.445 and 3.5 respectively, at P/e 10. The maximum thermohydraulic performance obtained is 2.3378 at the Reynolds number of 12000.

Key Words: CFD Simulation, Heat transfer, Solar air heater, Artificial roughness.

1. INTRODUCTION

A solar air heater is a form of solar thermal system in which air is heated in a collector and then transported to either the interior space or a storage medium. Solar collection panels, a duct system, and diffusers are the

essential components of a solar air heater. Because of its basic design, solar air warmers are among the most affordable and extensively used solar energy equipment. Solar air heaters have a variety of applications, including room heating, curing of industrial items, and curing/drying of concrete/clay building components. We know that the convective heat transfer coefficient between the air and the absorber plate in a solar air heater is quite low due to the low thermal conductivity of air [1]. In order to enhance heat transmission in the solar air heater, we must first improve heat transfer in the solar air heater. The study of heat transfer mechanisms and fluid flow is critical for improving performance in terms of improved thermodynamic efficiency and power production for heat exchanging devices such as solar air heaters and heat exchangers. The computational fluid dynamics (CFD) technique is less expensive than experimental research for evaluating the thermal performances of heat exchanging devices. The advantages of CFD are that we can make different complex geometries, different shape and sizes and can produce a large number of results at no added expense and it is very cost effective to perform parametric studies for optimization of the equipment performance.

There are several strategies for improving heat transmission in a solar air heater. However, boosting the heating capacity of the solar collector by adding artificial roughness to the absorber plate is the simplest and least expensive method [2].

Various researchers [2-4] investigated the forms and placements of ribs experimentally.

A 3D CFD analysis of heat transfer and fluid flow characteristics through an artificially roughened solar air heater with arc-shaped rib roughness was carried out by Kumar and Saini [5]. They offered the artificial roughness in the form of arc-shaped thin circular wire. They covered a wide range of roughness parameters (e/D from 0.0299 to 0.0426 and $a/90$ from 0.333 to 0.666) as well as operating parameters (Reynolds number, Re from 6000 to 18,000 and solar radiation of 1000 W/m²). Their maximal enhancement ratio value was 1.7. Karmare and Tikekar [6] performed a 3D CFD simulation of fluid flow and heat transfer in an intentionally roughened solar air heater with metal grit rib roughness. They created the roughness with metal ribs with round, square, and triangular cross-sections that were angled at 60 degrees to the air flow. They used the parameters: $e/D_h = 0.044$, $p/e = 17.5$ and $l/s = 1.72$, for the Reynolds number range 3600–17,000.

They discovered that the square plate had a 30% advantage over a smooth surface. Previous research looked at the roughness of a solar air heater duct with inclined discrete ribs. Then, inclined discrete rib roughness with rectangular shaped staggered element geometry was investigated. In this experiment, I'm altering the form of the staggered element. In this investigation, I will employ inclined discrete rib roughness with a staggered convex/concave element. According to the advice offered by increase in the heat transfer for intentionally roughened solar air heaters, the authors advised that the Renormalization group (RNG) k -model is the most appropriate turbulence model for modelling of artificially roughened solar air heaters [7].

In the present work a computational investigation of turbulent forced convection in a two-dimensional duct of a conventional solar air heater is conducted. The objectives of the present study are:

1. To develop a three-dimensional CFD model of a conventional solar air heater to obtain numerical predictions for heat transfer and fluid flow performance.
2. To investigate the predictive ability of Renormalized Group (RNG) k - ϵ turbulence model.
3. To compare the predicted results with past experimental data in order to validate the CFD model.
4. To compare the results obtained by changing the shape of the staggered element.

2. CFD Approach

Computational Fluid Dynamics (CFD) is a way of analysing fluid flow that use numerical solution methods. We may use CFD to solve complicated issues involving fluid-fluid, fluid-solid, or fluid-gas interaction. The current computational domain is the same as the one utilised by Rathor and Aharwal [8]. The approach is extremely effective and is utilised in a broad variety of industrial and non-industrial applications. CFD analysis saves time in the design process and is less expensive and faster than traditional data collecting tests. Furthermore, in experimental testing, only a limited number of values are measured at a time, but in a CFD analysis, all necessary quantities may be assessed at once and with great spatial and temporal resolution.

CFD analysis basically consists of the three phases:

Pre-processing - entails transforming the problem into an idealised and discretized computer model. Assumptions are made based on the type of flow being simulated. Following that, the mesh is generated and the initial- and boundary conditions are applied.

Solving - The solver then does the actual computations, and processing power is required during this step. There are several solvers accessible, each with varying degrees of efficiency and competence in addressing certain physical phenomena.

Post-processing - During the post-processing step, the generated data are viewed and analysed. The analyst can

review and validate the results in post processing, and conclusions can be taken based on the collected data. The obtained results can be presented by static or moving pictures, graphs or tables.

CFD programmes are built around numerical techniques that handle fluid flow issues. To facilitate access to their computational capability, all commercial CFD software feature sophisticated user interfaces for entering issue parameters and seeing the results.

The investigation of a 3-dimensional CFD simulation of a standard solar air heater. As a solver, the commercial CFD simulation code FLUENT (version R1 2021) is employed. For analysis, the following assumptions are employed.

1. The flow is continuous, fully developed, turbulent, and three-dimensional.
2. The thermal conductivity of the absorber plate, duct walls, and roughness material is temperature independent.
3. The duct wall and absorber plate are isotropic and homogenous.
4. The walls in contact with the fluid are subjected to a no-slip boundary condition.
5. Minimal heat transfer and other heat losses due to radiation.

3.1 Model Development

As shown in fig. 1, the suggested 3-D computational domain for CFD analysis has a height of 40 mm, a width of 200 mm, and a length of 1630 mm. The duct geometry is separated into three sections: the input part, the test section, and the exit section. The lengths of the inlet and exit sections are chosen in accordance with ASHRAE standards [9], i.e., the inlet section length should not be less than $5(WH)^{0.5}$ for flow development and the length of the outlet section should be at least $2.5(WH)^{0.5}$ to limit its end impacts. As a result, the lengths of the input section, test section, and exit section are 470 mm, 900 mm, and 260 mm, respectively. In this work, inclined discrete ribs with staggered components are used as roughness elements to improve heat transmission. The staggered element is created in a variety of forms. The ribs are formed on the underside of the top plate, while the other sides are smooth. The height of the ribs is set at 2 mm so that the obstruction impact of the ribs is insignificant, and the pitch is set to 12-24 mm.

Table -1: Geometric and Operational parameters for Computational analysis.

Geometric and Operational Parameters	Range
Entrance length of duct, ' L_1 '	470 mm
Test length of duct, ' L_2 '	900 mm
Exit length of duct, ' L_3 '	260 mm
Width of duct, ' W '	200 mm
Height of duct, ' H '	40 mm
Hydraulic diameter of duct, ' D_h '	66.66 mm
Duct aspect ratio, ' W/H '	5
Rib height, ' e '	2 mm
Relative roughness height, ' e/D_h '	0.03
Uniform heat flux, ' I '	$820 W/m^2$
Reynolds Number, ' Re '	6000-12000
Prandtl Number, ' Pr '	0.71

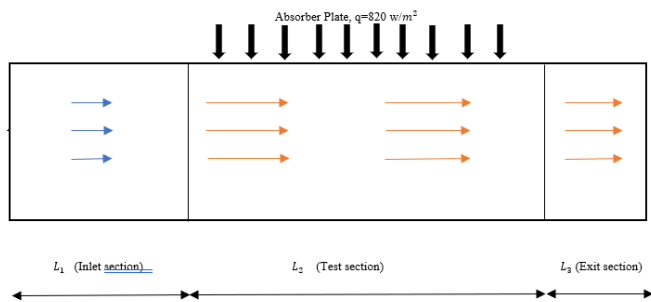


Fig. 1. 2-D computational domain

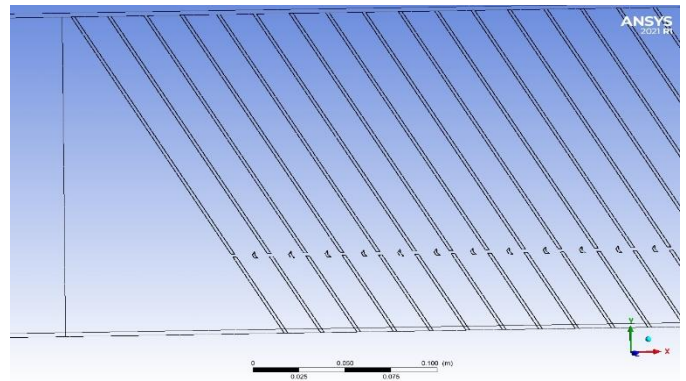


Fig. 3. Inclined rib with convex element CFD geometry

3.2 Mesh Generation

Meshing is completed after the geometry has been created. For the whole domain, a uniform tetrahedral mesh element is chosen, and a uniform mesh is created throughout the entire model. There are more cells near the absorber plate in this mesh to resolve the turbulent boundary layer, which is quite thin in comparison to the height of the flow field. The grid independence test has been completed. After meshing, there are 1061307 nodes and 5564941 elements.

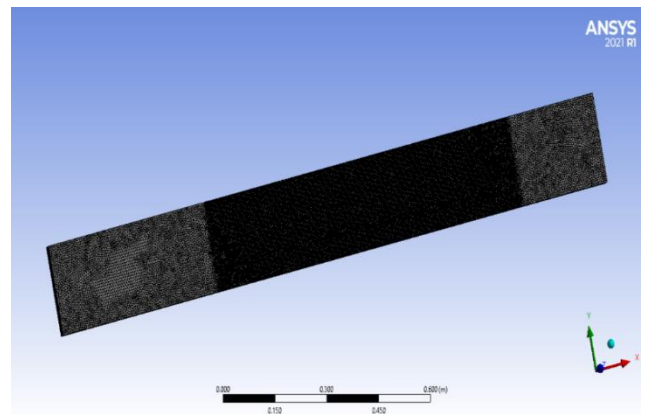


Fig. 4. Meshed model with tetrahedral elements

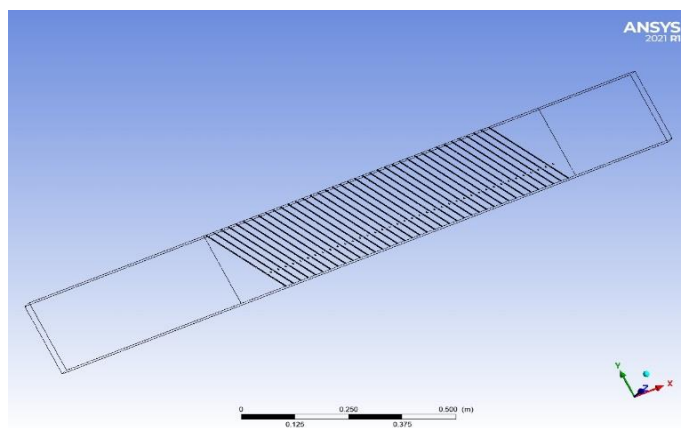


Fig. 2. Model Geometry in Ansys Design modeler

3.3 Boundary Conditions

The boundary conditions are as follows:

1. Inlet velocity
2. The duct's hydraulic diameter (fixed)
3. Fixed outlet pressure Pressure in the atmosphere)
4. Constant heat flux on the test section's absorber plate
5. There is no heat transmission from the duct's other walls.

Table 2. Details of boundary conditions.

Edge Position	Name	Type
Left	inlet	Velocity
Right	outlet	Pressure
Top entrance wall	wall	Wall
Top exit wall	wall	Wall
Top test wall	Heater	Wall
Bottom wall	wall	Wall

Table 3. Thermo-physical properties of working fluid (air) and absorber plate (aluminium) for CFD analysis.

Properties	Working fluid (air)	Absorber plate (aluminium)
Density ' ρ ' (kg/m^3)	1.225	2719
Specific heat ' C_p ' ($Jkg^{-1}k^{-1}$)	1006.43	871
Dynamic viscosity ' μ ' ($Nm^{-2}sec$)	1.7894e-05	-----
Thermal Conductivity ' k ' ($Wm^{-1}K^{-1}$)	0.0242	202.4

3.5 Solver

The equations are solved using Ansys FLUENT R1 2021. All governing equations (Continuity, Momentum, and Energy) are discretized using a finite volume technique by a second order upwind-biased scheme and then solved separately. To associate pressure and velocity for the incompressible flow computation, the SIMPLE (semi-implicit technique for pressure linked equations) algorithm is used [12]. For the modelling of fluid flow and heat transport properties, the RNG k-epsilon turbulence model was chosen [13]. The RNG turbulence model takes into account the top regime with little or no impact from the buffer area. This model exhibits turbulent flow with high anisotropy. The convergence criteria of 10^{-6} for the residuals of the continuity equation, 10^{-6} for the residuals of the momentum the equation, 10^{-3} for the residuals of the velocity components and 10^{-6} for the residuals of the energy equation is assumed.

4. Data Reduction

I. Heat gain from heated surface,

$$Q = \dot{m}C_p(T_o - T_i) \tag{1}$$

Where, $\dot{m} = \rho AV$

II. Heat transfer coefficient,

$$h = \frac{Q}{A(T_{mp} - T_{mf})} \tag{2}$$

III. Nu and f are estimated by the following equations,

$$Nu = \frac{hD_h}{k} \tag{3}$$

$$\text{And } f = \frac{\Delta P D_h}{2\rho LV^2} \tag{4}$$

ΔP can be calculated by CFD simulation.

Nu_s and f_s for smooth surface can be calculated from following equations:

Dittus-Boelter eqn. [10]

$$Nu_s = 0.023Re^{0.8}Pr^{0.4} \tag{5}$$

Blasius eqn. [11]

$$f_s = 0.079Re^{-0.25} \tag{6}$$

Thermal hydraulic performance can be calculated by:

$$THPP = \frac{Nu/Nu_s}{[f/f_s]^{1/3}} \tag{7}$$

5. CFD Results

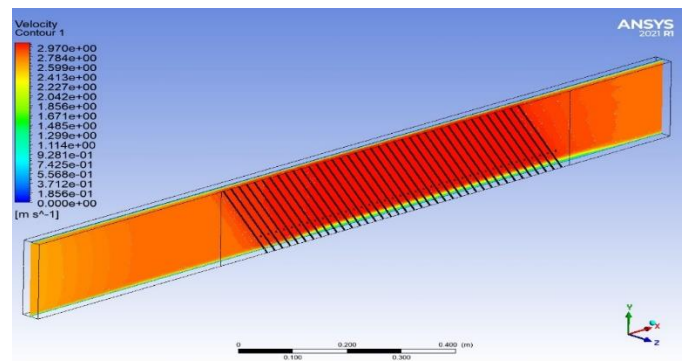


Fig. 5. Velocity contour for convex element at 12000 Re

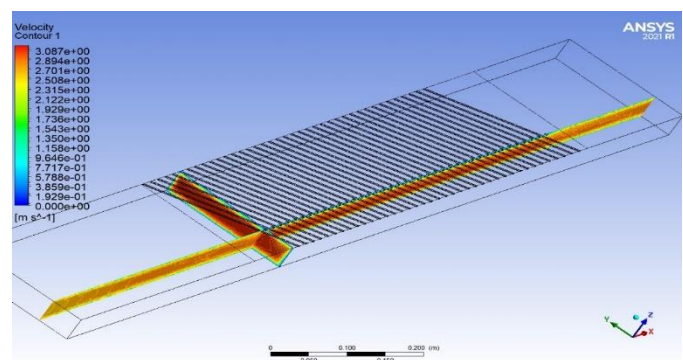


Fig. 6. Velocity contour in X and Y plane at 12000 Re

Fig. 5 and 6 shows the velocity contours of the solar air heater geometry for inclined ribs with convex staggered element at 12000 Reynolds number.

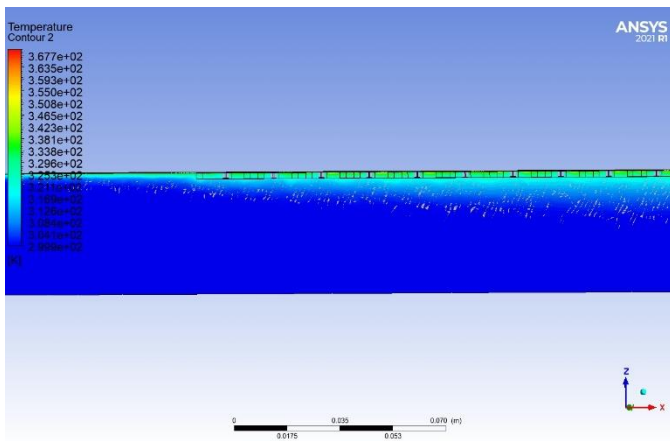


Fig 7. Temperature contour in Y plane at 12000 Re

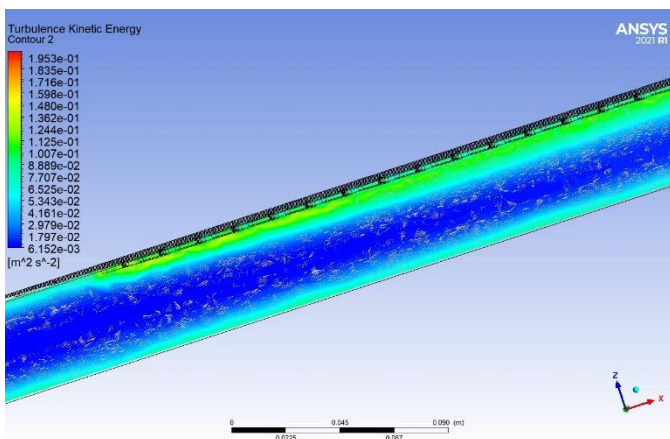


Fig. 8. Turbulent kinetic energy contour for the plate

Fig. 7 and 8 shows the Temperature contour and Turbulent kinetic energy contour respectively for the proposed geometry obtained by CFD simulation.

The following charts shows the results obtained from the CFD simulation for the geometries.

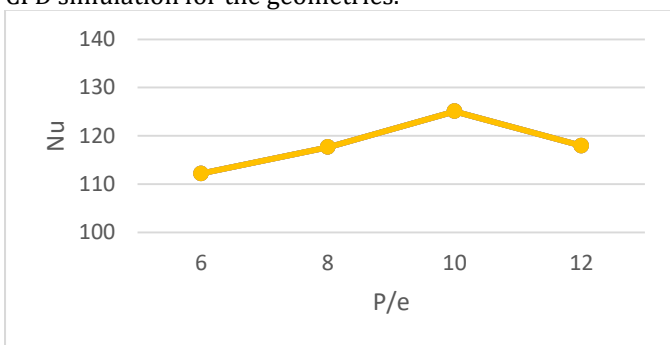


Chart 1. Nu vs P/e for various Reynolds number for Convex element.

Chart 1 shows that the value of Nu number increases as the Re number increases for all values of P/e because the turbulence intensity increases as the value of Re number increases. It can be seen that in chart 1 the Nu number is

highest at P/e = 10 at all values of Re. After that Nu decreases for all values of Re.

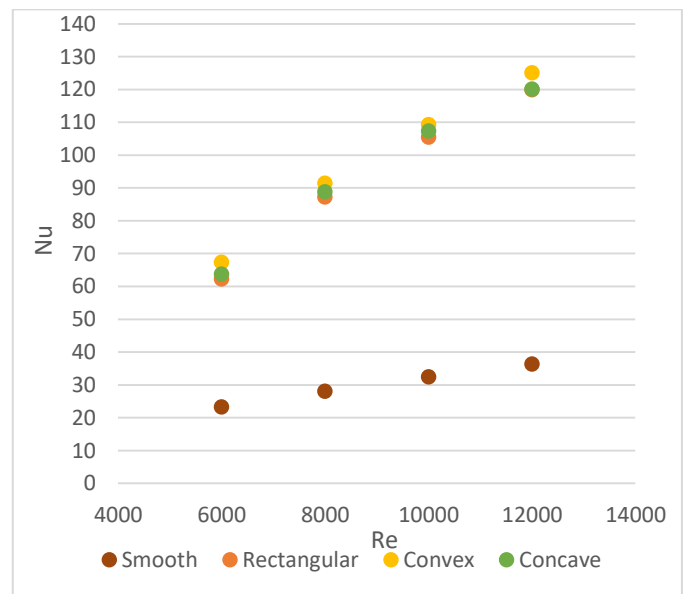


Chart 2. Nu vs Re for various shaped element at P/e 10

Chart 2 compares the Nu for all Re values at P/e 10 of the proposed roughness geometry with inclined discrete rib, Rectangular shaped staggered element, Concave shaped staggered element, and smooth surface. It can be seen that the value of Nu is highest for all values of Re at P/e 10 because the turbulence intensity is higher due to the convex shaped element, which increases the value of heat transfer coefficient, and thus the value of Nu is higher for convex shaped staggered element as compared to other shapes.

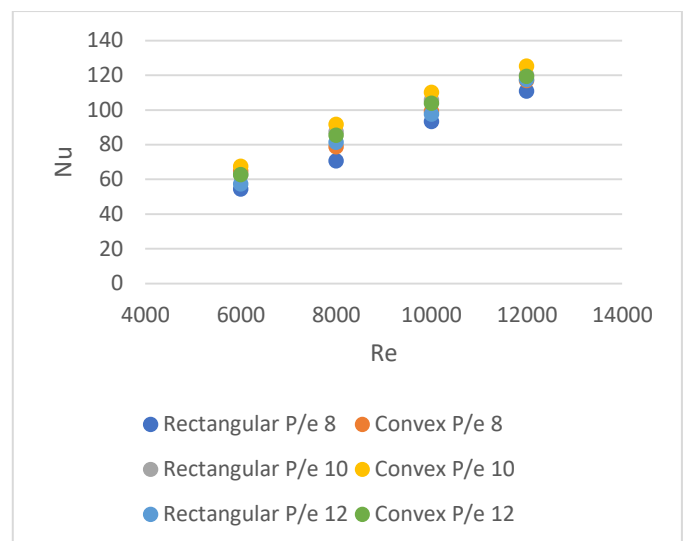


Chart 3. Nu vs Re for Rectangular and Convex element at various P/e

Chart 3 shows the comparison of the Nu for all values of Re for the Rectangular shaped and Convex shaped

staggered element. As we have already seen that the Nu is highest at P/e 10 and for Convex element for all values of Re. The reason being that the turbulence intensity increases more in convex element as compared to rectangular element.

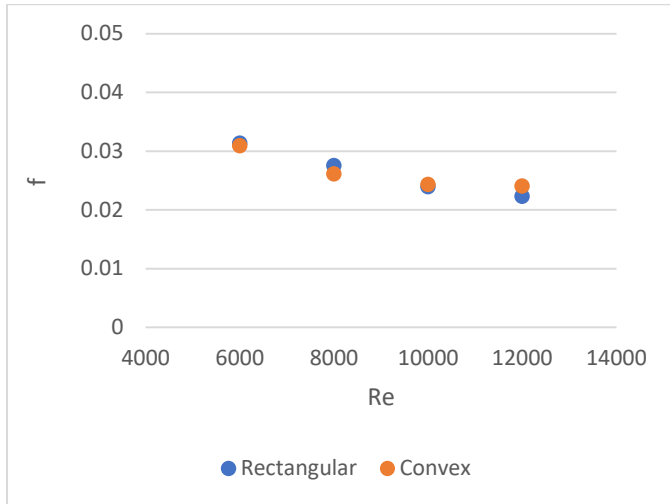


Chart 4. Re vs f for elements at various Reynolds number.

Chart 4 shows the f variation for all values of Re at P/e 10. It can be seen that the f decreases as the Re increases. After 8000 Re the friction is more for convex element than for rectangular element. This is because as the Re increases the boundary layer diminishes hence the resistance in flow also decreases hence the friction decreases.

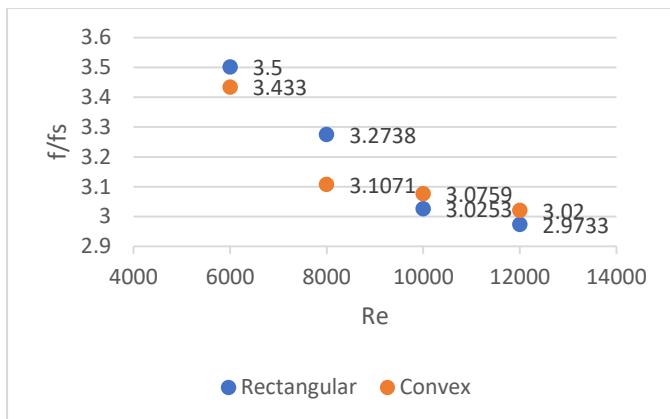


Chart 5. Re vs f/fs for elements for different Reynolds number.

Chart 5 shows the friction factor ratio for geometry with staggered element and the smooth surface for all values of Re at P/e 10. The maximum value of the friction factor ratio is obtained at 6000 Re of 3.5. It further decreases as the value of Re increases.

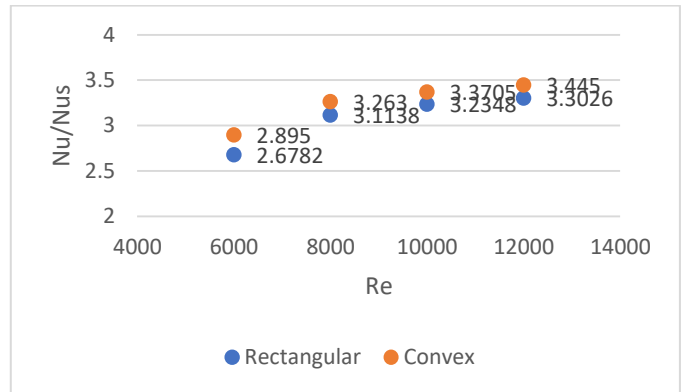


Chart 6. Re vs Nu ratio for elements for various Reynolds number.

The comparison of the augmentation in heat transmission of suggested roughness geometry with inclined discrete rib with rectangular element and convex element is shown in Chart 6. It demonstrates that when Re grows, so does the Nu/Nu_s ratio. It might be because when the working fluid flows from the leading edge to the following edge along the rib, the flow gradually heats up and the boundary layer thickens. The gap along the trailing edge allows the secondary flow to be released concurrently with the primary flow, accelerating it and increasing the heat transfer capacity. The staggered element improves the turbulence intensity and helps to reinforce the surrounding region, resulting in increased heat transfer.

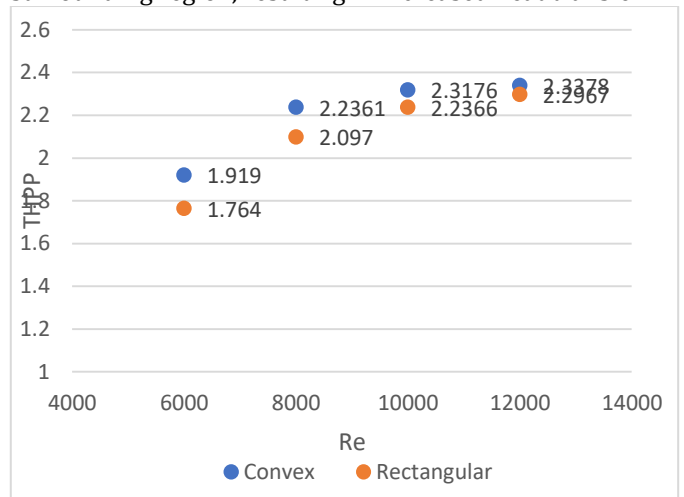


Chart 7. THPP vs Re for elements for various Reynolds number.

Chart 7 compares the THPP of convex and rectangular staggered elements for various Re values. The combined impact of Nu and f is essential for THPP assessment. As a result, testing the thermo-hydraulic performance characteristic of SAH is required to determine the ideal rib pitch at which Nu is maximal with minimal f. To improve the THPP, the Nu should be as high as possible and the f should be as low as possible. THPP should be bigger than one to guarantee that the roughness geometry is beneficial. As a result, it may be used to compare different

roughness geometries. The greatest THPP value obtained at P/e 10 and 12000 Re is 2.3378.

6. Model Validation

The results obtained are verified by Rathor and Aharwal's experimental study [8]. There was some fluctuation in the results. The difference between the present CFD result and the experimental data set is 10%. The current analysis demonstrates a significant agreement with the experimental data set.

7. Conclusions

In this present investigation, a numerical prediction has been conducted to study heat transfer and flow friction behaviours of a rectangular duct of a solar air heater having inclined discrete rib with rectangular and convex staggered element roughness on the absorber plate. The main conclusions are:

1. There is no question that one of the primary goals of CFD analysis of solar air heaters is to improve the design process that deals with heat transfer and fluid flow.
2. CFD has recently been used in the design of solar air heaters. The quality of the solutions generated from CFD simulations is often within acceptable limits, demonstrating that CFD is an excellent technique for forecasting the behaviour and performance of a solar air heater.
3. The Nusselt number rises as the Reynolds number rises.
4. Solar air heater with inclined rib roughness having convex staggered element provides better heat transfer than rectangular staggered element.
5. The greatest Nusselt number for a convex-shaped staggered element with a pitch of 10 has been discovered.
6. The THPP of 2.3378 was obtained for the convex staggered element.

REFERENCES

- [1] A.S. Yadav, J.L. Bhagoria, Renewable energy sources-an application guide: energy for future, Int. J. Energy Sci. 3 (2) (2013) 70–90
- [2] J. Nikuradse, Laws of flow in rough pipes, VDI Forsch 361 (1933). English translation. National Advisory Committee for Aeronautics, Technical Memorandum 1292, 1950.
- [3] A.S. Yadav, V. Shrivastava, M.K. Dwivedi, O.P. Shukla, 3-dimensional CFD simulation and correlation development for circular tube equipped with twisted tape, Materials Today: Proceedings (2021), <https://doi.org/10.1016/j.matpr.2021.02.549> In press.
- [4] W. Nunner, Heat transfer and pressure drop in rough pipes, AERE Lib/Trans. 786 (1958).
- [5] Kumar, S., and R. P. Saini. 2009. "CFD Based Performance Analysis of a Solar Air Heater Duct Provided with Artificial Roughness." Renewable Energy 34 (5): 1285–1291. <https://doi.org/10.1016/j.renene.2008.09.015>.
- [6] Karmare, S. V., and A. N. Tikekar. 2010. "Analysis of Fluid Flow and Heat Transfer in a Rib Grit Roughened Surface Solar Air Heater Using CFD." Solar Energy 84 (3): 409–417. <https://doi.org/10.1016/j.solener.2009.12.011>.
- [7] A.S. Yadav, J.L. Bhagoria, Heat transfer and fluid flow analysis of solar air heater: a review of CFD approach, Renew. Sustain. Energy Rev. 23 (2013) 60– 79.
- [8] Yogendra Rathor, KR Aharwal, Heat transfer enhancement due to a staggered element using liquid crystal thermography in an inclined discrete rib roughened solar air heater, International Communications in Heat and Mass Transfer 118 (2020) 104839. <https://doi.org/10.1016/j.icheatmasstransfer.2020.104839>
- [9] ASHRAE standard 93-97, Method of Testing to Determine the Thermal Performance of Solar Collectors, American Society of Heating, Refrigeration and Air Conditioning Engineers, New York (1977).
- [10] S. Patankar, Numerical Heat Transfer and Fluid Flow, CRC Press, 1980.
- [11] W.H. McAdams, Heat Transmission, McGraw-Hill Book Co., New York, 1942.
- [12] R.W. Fox, A.T. McDonald, P.J. Pritchard, Introduction to Fluid Mechanics, John Wiley & Sons New York, 1985.
- [13] A review on selection of turbulence model for CFD analysis of air flow within a cold storage by Pankaj Mishra and K R Aharwal. IOP Conf. Series: Materials Science and Engineering 402 (2018) 012145 <https://doi.org/10.1088/1757-899X/402/1/012145>.

AUTHOR PROFILES

Mahendra Kumar Ahirwar,
Engineering graduate specialized
in Mechanical Engineering.
Currently pursuing M.Tech in
Thermal Engineering from
MANIT Bhopal, MP, India.



Dr. K.R. Aharwal,
Highest qualification Phd. His
research area is thermal
engineering. Currently a
Professor in Department of
Mechanical Engineering in
MANIT Bhopal,MP, India.